Journal of Seismology **6**: 219–236, 2002.

S-wave spectral analysis of the 1995 Kozani-Grevena (NW Greece) aftershock sequence

Zafeiria Roumelioti[1], Anastasia Kiratzi[1], Nikos Theodoulidis[2] & Christos Papaioannou[2]
[1]*Department of Geophysics, Aristotle University of Thessaloniki, 54006, Thessaloniki, Greece (e-mail: zroum@lemnos.geo.auth.gr);* [2]*Institute of Engineering Seismology and Earthquake Engineering, P.O. Box 53, 55102, Thessaloniki, Greece*

Received 29 August 2000; accepted in revised form 12 January 2001

Key words: Aegean, source parameters, spectral analysis

Abstract

S-wave spectral analysis is applied to 174 strong motion acceleration records to obtain the source parameters of 27 aftershocks ($3.1 \leq M_L \leq 4.3$) of the May 13, 1995, M_w 6.6, Kozani-Grevena (NW Greece) earthquake. The data are derived from a temporary network, of three-component digital accelerographs, deployed within the strongly affected area some days after the mainshock occurrence. Site effects were evident in the strong motion records at 3 out of the 4 stations used, and a correction was applied to account for the overestimation of seismic moment due to amplification of the low-frequency part of the spectrum. The data from this analysis are complimented with previously obtained source parameters for earthquakes in Greece, in order to study the applicability of the empirical scaling relations used so far, towards smaller magnitudes. In general, a good correlation was observed in most cases, validating the use of empirical relations that are applicable to the Aegean area. Empirical relations are determined between seismic moment and seismic slip, as well as, between seismic moment and stress drop, applicable to small magnitude earthquakes ($M_L < 4.3$). Stress drop values were found to be relatively small, ranging from 2 to 41 bars, indicative of inter-plate environments. The values of f_c and of f_{max} were found in good agreement with relations based on observations from larger worldwide earthquakes.

Introduction

On May 13, 1995, a destructive earthquake (M_w 6.6) occurred at northwestern Greece (Kozani prefecture) and caused extensive damage in many villages and in the two large towns of the area, Kozani and Grevena. A few days after the mainshock, the Institute of Engineering Seismology and Earthquake Engineering (ITSAK) installed a temporary network of three-component digital accelerographs (SSA-1, 2) within the meizoseismal area.

From a considerable number of aftershocks recorded on the local accelerometer network, only 27 (those that were recorded at more than three stations) were chosen for an analysis of their source parameters. The main purpose of this analysis was to examine the validity of the self-similarity law of small-magnitude earthquakes of the area, through a comparison of the extracted values with regional or global relations proposed for larger magnitude earthquakes. If self-similarity law is valid for the study area then source parameters of small earthquakes could be estimated from a simple extrapolation of the relations that hold for large earthquakes, otherwise local relations should be determined.

The source parameters were determined using spectral analysis (Brune, 1970, 1971), which is a method widely applied. In Greece, this method has been repetitively applied, mainly for the estimation of source parameters of microearthquakes (e.g., Burton et al., 1991; Melis et al., 1995; Chouliaras and Stavrakakis, 1997). Comparison of the estimated source parameters of small magnitude earthquakes ($3.1 \leq M_L \leq 4.3$) with relevant parameters of larger earthquakes ($M_L \geq 4.0$) is attempted and discussed.

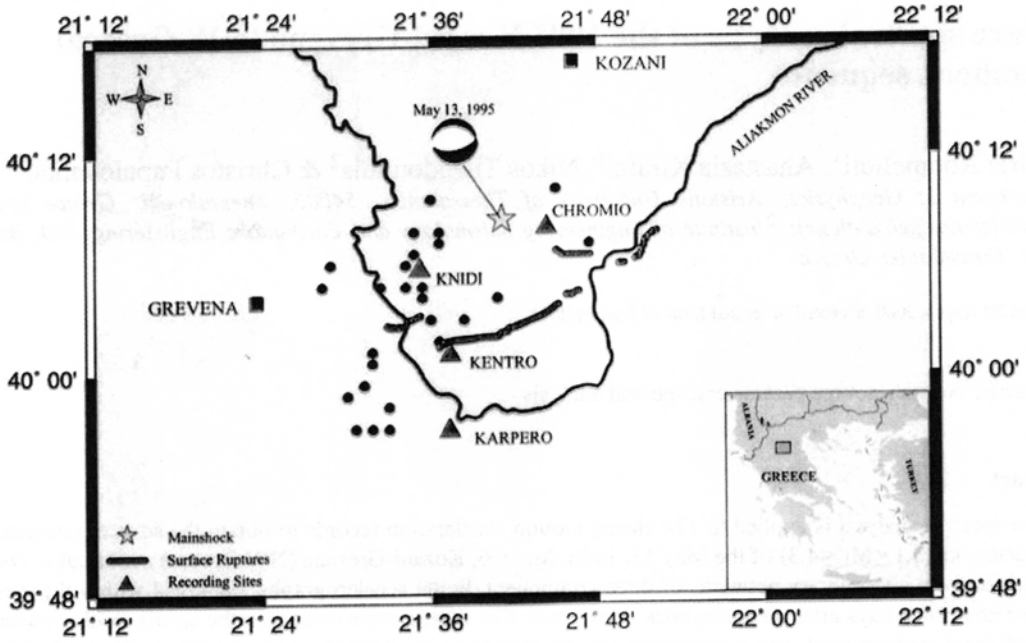

Figure 1. Regional map showing the May 13, 1995 Kozani mainshock (star), the epicenters of the 27 aftershocks analyzed (solid circles) and the locations of the four accelerometer stations (triangles). The solid thick line represents surface ruptures observed after the mainshock (Pavlides et al., 1995).

Data analysis

The original data set consists of 174 horizontal accelerograph components, as each one of the 27 selected earthquakes was at least recorded at three stations. These records are sampled at a rate of 200 Hz and their bandwidth is 0.3 to 45 Hz. Local magnitudes range from 3.1 to 4.3, while hypocentral distances are between 4 km and 28 km. The values of M_L presented in this paper, are taken from the catalogue proposed by Baba et al. (2000) towards a unified M_L for the South Balkan area. Figure 1 shows the epicentres of the analysed earthquakes, as well as the epicentre of the mainshock, its surface ruptures (Pavlides et al., 1995) and the locations of the four accelerograph stations used. Table 1 gives information on the earthquakes used and lists the source parameters of the aftershocks obtained in this study.

Following Brune (1970, 1971), the displacement spectrum of ground motion of an earthquake can be described by a straight line that fits the low-frequency level of the spectrum, intersecting the high-frequency asymptote at the corner frequency, f_c. The low-frequency asymptotic displacement, Ω_0, is proportional to seismic moment, M_0, while the corner frequency, f_c, is inversely proportional to the radius of the circular fault considered by the model.

To apply the S-wave spectral analysis an appropriate time window of S-waves must be selected. According to a large number of previous studies (e.g., Thatcher and Hanks, 1973; Modiano and Hatzfeld, 1982; Archuleta et al., 1982; Meuler and Cranswick, 1985; Del Pezzo et al., 1987; among others), for hypocentral distances <40 km, as those of the 27 earthquakes used in this work and for magnitudes within the examined range, the length of the chosen time windows can vary from 1s–3.5s without practically changing the low-frequency level of the spectrum or the choice of the corner frequencies. Tests (comparisons of spectra derived from the use of different S-wave window lengths) conducted to our data, confirmed this deduction. As a result, the selected time windows, for this study, started slightly before the S-waves and their duration varied, from record to record, from 2.5 s to 3.5 s, as we tried to encompass the

complete displacement pulse (Archuleta and Hartzell, 1981).

The displacement amplitude spectrum of each one of the two horizontal components, at each recording station, was computed by applying Fast Fourier Transform (FFT) to the corresponding time window, and the output of the Fourier transform was post- multiplied by f^{-2} to obtain the displacement spectrum. The value of Ω_0 was determined by eye fitting a straight line to the low-frequency part of the spectrum.

The displacement spectra were not corrected for the effect of whole path attenuation (Q), since this effect is expected to be negligible (Archuleta et al., 1982), especially at epicentral distances less than 50 km (Street et al., 1975).

The low-frequency level, Ω_0, is connected to seismic moment, M_o, through the empirical relation (Keilis-Borok, 1959):

$$M_0 = \frac{4\pi\rho R\beta^3\Omega_0}{kR_{\theta\phi}} \tag{1}$$

where ρ is density, R is the source-to-recorder distance, β is the shear wave velocity at the source, k is a correction factor for free surface reflection and $R_{\theta\phi}$ is the S-wave radiation pattern coefficient. Usually, the product $kR_{\theta\phi}$ is given a mean value of 0.85, which was also adopted here.

Seismic moments were determined from means of the logarithmic values obtained at different stations, as proposed by Archuleta et al. (1982), following the equation:

$$M_0 = \text{antilog}\left\{\frac{1}{N}\sum_{i=1}^{N}\log M_{0i}\right\} \tag{2}$$

where N (= Number of stations $\times$ 2) is the number of the components used and M_{0i} is the seismic moment determined from (1), for the i^{th} record.

The spectral corner frequency, f_c, was determined from the intersection of the high-frequency asymptote with the low-frequency asymptote of the spectrum. We followed the approach of Bour (1989), based on the work of Andrews (1986), and we automatically estimated the corner frequencies, f_c. All values of f_c were visually checked both on displacement and on acceleration amplitude spectra of each S-wave time window used. Average values of f_c for each earthquake were determined by an equation analogous to (2). This equation, as well as those used for the computation of the seismic moment and corner frequency error factors (EM_0 and Ef_c, correspondingly) are taken from Archuleta et al. (1982).

The average values of the corner frequency, f_c, were used for estimating the radii of the seismic sources, following the model of Brune (1970,1971). According to this model, the radius, r, for a circular fault rupture, is given by:

$$r = \frac{0.37\beta}{f_c} \tag{3}$$

where β is the S-wave velocity.

The average values of M_0 and r, determined as described above, were used for the estimation of average stress drop, $\Delta\sigma$, from the equation:

$$\Delta\sigma = \frac{7M_0}{16r^3} \tag{4}$$

(Keilis-Borok, 1959) as well as for the estimation of the average coseismic slip, s, over the circular fault area from the equation:

$$s = \frac{M_0}{\pi r^2\mu} \tag{5}$$

(Brune, 1968) where μ is the rigidity modulus of the fault material.

The cut-off frequency, f_{max}, was also determined from the Fourier spectra of strong motion acceleration recordings. f_{max} is the frequency up to which the acceleration spectrum is flat and above which a spectral roll-off is observed (Hanks, 1979). This sharp diminution of the acceleration spectrum is attributed either to the source rupture process (Papageorgiou and Aki, 1983; Aki, 1987; Papageorgiou, 1988) or to the anelastic attenuation along the travel path (Hanks, 1979) or to near-surface attenuation (Hanks, 1982; Anderson and Hough, 1984; Theodoulidis and Bard, 1998). Thus, it has not been clear yet whether f_{max} consists a source parameter or not. Nevertheless, it consists a parameter of great importance, as it is directly related to engineering measures of high-frequency ground motion (Papageorgiou, 1988).

The values of f_{max} were automatically estimated using the method of Bour (1989). This method includes semi-analytical and numerical estimations of f_{max} based on the Brune's model (1970, 1971) and semi-analytical estimations based on the model of Anderson and Hough (1984). The automatically estimated values of f_{max} were also checked visually on the acceleration spectrum of each component used.

An example of the Ω_0, f_c and f_{max} estimation (Event 25 in Table 1) is given in Figure 2.

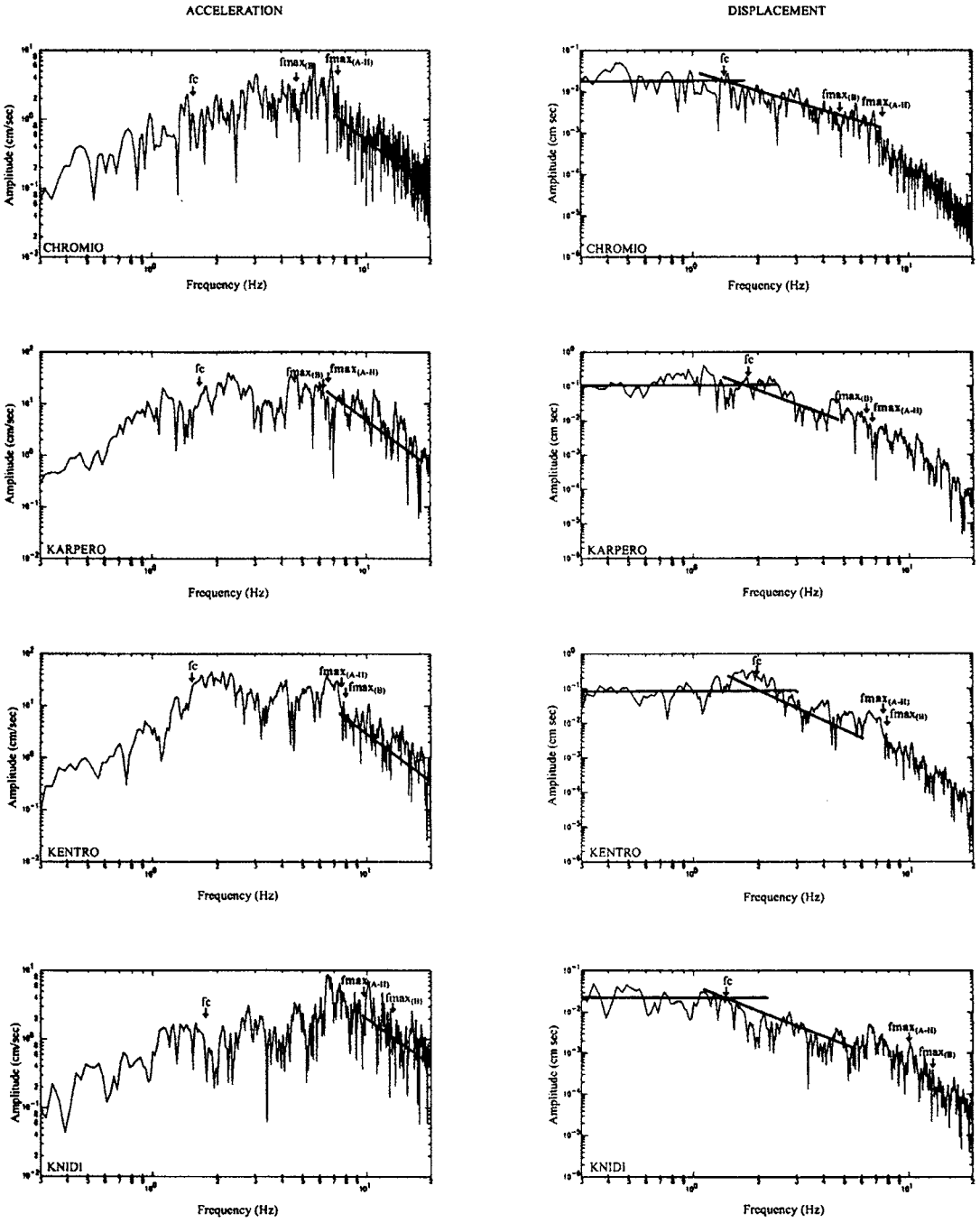

Figure 2. An example of the Ω_0, f_c and f_{max} estimation from the acceleration and displacement Fourier amplitude spectra, at four different recording stations (Event 25 in Table 1, longitudinal component). The automatically estimated values of f_{max} based on Brune's model ($f_{max(B)}$) and on the Anderson and Hough (1984) model ($f_{max(A-H)}$) are both shown. The selected values of f_{max} appear in bold letters.

Table 1. List of earthquakes analysed in this study together with their epicentral coordinates, depth (h), local magnitude (M_L) and number of recording stations (NS). Estimated average source parameters (seismic moment M_0 and its error EM_0, corner frequency f_c and its error Ef_c, source radius, r and stress drop, $\Delta\sigma$) are also listed. All epicentres and focal depths are determined by the Geophysical Laboratory of the University of Thessaloniki. Local magnitudes, M_L, are taken from the catalogue proposed by Baba et al. (2000)

Event No	Date	Or. Time	Lat. (N)	Long. (E)	h (Km)	M_L	M_o ($*10^{21}$) (dyn·cm)	EM_o	f_c (Hz)	Ef_c	r (Km)	$\Delta\sigma$ (bars)	NS
1	950523	05:51:59	40.17	21.75	12.8	3.9	5.1	1.25	2.0	1.22	0.64	8	3
2	950524	16:18:55	40.08	21.59	5.5	3.2	2.3	1.36	1.9	1.15	0.66	3	3
3	950524	17:34:27	40.07	21.59	6.6	3.8	12.4	1.36	1.6	1.29	0.77	12	3
4	950524	19:29:06	40.08	21.59	6.0	3.1	1.7	1.10	1.7	1.49	0.74	2	3
5	950524	21:22:43	40.08	21.54	6.8	3.2	1.6	1.19	2.3	1.23	0.55	4	3
6	950525	01:40:27	40.05	21.60	6.6	3.2	1.0	1.75	2.3	1.09	0.54	3	3
7	950525	04:05:44	39.99	21.52	6.5	3.5	3.1	1.18	2.2	1.17	0.57	7	3
8	950525	04:35:07	40.08	21.57	7.6	3.2	2.2	1.42	2.4	1.21	0.53	6	3
9	950525	08:48:54	40.07	21.68	8.7	3.3	1.8	1.44	2.1	1.13	0.60	4	4
10	950525	21:37:20	40.03	21.61	7.2	3.2	2.2	1.60	2.3	1.21	0.55	6	3
11	950525	23:12:16	40.12	21.79	12.1	3.3	3.6	1.34	2.1	1.19	0.60	7	3
12	950527	05:52:56	40.01	21.53	14.9	3.3	3.1	1.23	2.1	1.20	0.61	6	3
13	950530	06:21:06	40.08	21.47	13.1	3.3	2.6	1.35	2.2	1.03	0.57	6	3
14	950530	06:46:00	40.10	21.48	9.9	3.8	2.8	1.55	2.1	1.28	0.59	6	3
15	950530	12:06:42	40.05	21.64	4.0	4.1	12.8	1.41	1.9	1.59	0.65	20	4
16	950530	14:30:02	39.97	21.55	6.2	4.0	12.2	1.19	1.8	1.33	0.71	15	3
17	950601	10:17:28	39.98	21.50	9.2	3.4	2.7	1.44	1.9	1.12	0.65	4	3
18	950602	07:47:15	40.02	21.53	3.4	3.5	3.6	1.11	1.7	1.45	0.75	4	3
19	950603	10:20:14	40.11	21.58	6.6	3.8	3.4	1.01	2.1	1.19	0.59	7	4
20	950606	00:46:52	40.16	21.60	11.3	3.6	2.8	1.37	2.2	1.13	0.57	7	3
21	950606	04:35:59	40.13	21.58	6.5	4.2	25.9	1.42	1.6	1.22	0.79	23	4
22	950607	08:37:34	40.10	21.57	3.4	3.9	6.7	1.80	2.0	1.13	0.64	11	3
23	950609	15:20:48	40.12	21.61	2.5	3.7	7.0	1.46	1.5	1.35	0.83	5	4
24	950611	17:20:10	40.13	21.61	1.5	3.8	4.5	1.29	1.8	1.27	0.70	6	3
25	950611	18:51:47	39.95	21.53	4.5	4.3	39.7	1.33	1.7	1.17	0.75	41	4
26	950611	20:38:22	39.95	21.55	5.0	3.6	3.8	1.13	1.9	1.16	0.65	6	3
27	950612	03:19:50	39.95	21.51	11.0	3.3	2.8	1.39	2.1	1.10	0.60	6	3

Results and comparisons

Estimation of seismic moment, M_o

In order to invert a displacement spectrum for source parameters, one must know or make reasonable assumptions about the attenuation factor Q, the elastic parameters of the medium and the site effects at the recording station (Scherbaum, 1994). The basic problem that we had to deal with was the elimination of site effects, since most of the recordings were obtained at sites that could hardly be characterized as rock-sites. Indeed, after an initial estimation of M_0, following the method described above, we observed a systematic difference in the values obtained for the same earthquake, at different stations. For example, the values obtained from the displacement spectra in Karpero were always larger compared to the corresponding values of the other three stations. On the other hand, the values of M_0 obtained from the recordings of Knidi station were always the lowest.

Table 2. Information on the four recording sites. Shear wave velocities are taken from Pitilakis et al. (1996)

Recording site	Vs_{30} (m/sec)	PGV_{max}/PGA_{max}
Chromio	640	28.9
Karpero	–	42.8
Kentro	320	40.4
Knidi	1040	19.7

After examining the available geological and geotechnical information on the epicentral area (Pitilakis et al., 1996), we attributed these differences to site effects. For example, the values of shear-wave velocity averaged over the top 30 m, near the recording sites (Table 2) are indicative of the existence of rock-site characteristics only under the station of Knidi. Indeed, except from the geotechnical indications, the accelerograms in Knidi are characterized by short durations and enrichment in high frequencies. Furthermore, an application of the horizontal-to-vertical spectral ratio technique (Theodoulidis et al., 1998) revealed that Karpero, Chromio and Kentro favour resonance between 0.5 Hz and 2.5 Hz, which implies thicker and/or softer soil deposits under these stations, while Knidi favours resonance at much higher frequencies (2.5 Hz-8.0 Hz). In addition, the ratio of horizontal peak ground velocity to horizontal peak ground acceleration (PGV_{max}/PGA_{max}, in Table 2) exhibits considerably lower values in Knidi compared to the other three stations. This could also be an indication of the existence of rock-site conditions in Knidi, if we assume that the variation of this ratio with local geological conditions, estimated by Seed et al. (1976) for moderate magnitude earthquakes, holds also for small earthquakes.

In order to check the difference in the level of the estimated seismic moment, we plotted the values of $\log(M_0)$ against M_L, for each station separately (Figure 3). It appears that data can be described by a general equation of the form:

$$\log M_0 = aM_L + b_{station} \quad (6)$$

The slope, a, of the least squares' fit at the four data sets appears to be practically the same and almost equal to 1, while there is an obvious difference in the values of parameter $b_{station}$. A slope equal to 1 is also theoretically expected for earthquakes with corner frequencies greater than the cut-off frequency of the Wood-Anderson seismograph (1.25 Hz) (Randall, 1973; Archuleta et al., 1982; Fletcher et al., 1984).

We assumed a common slope for all stations, fixed at the value of 1, recalculated the values of the parameter b and extracted a mean $b_{station}$ for each site. The initial values of $\log(M_0)$ obtained in Karpero, Chromio and Kentro were reduced by the difference $b_{station}-b_{Knidi}$. The values of $\log(M_0)$ before the correction for site effect (open squares) are plotted in Figure 3, together with the reduced values accounting for the amplification of the low-frequency part of the spectrum (solid squares). The final mean values of the seismic moment, M_0, of the 27 earthquakes (Table 1) were estimated from equation (2). A least squares' fit to the reduced data from all stations yields a relation of the form: $\log(M_0) = (0.99\pm0.04)M_L + (18.1\pm0.15)$. This relation holds for earthquakes with magnitudes less than 4.3.

Table 3. Values of f_{max} obtained from the mean of the two horizontal components at the different stations

Event No	f_{max} Chromio	Kentro	Karpero	Knidi
1	11.0	6.0		7.8
2		6.9	6.9	9.5
3		5.9	7.4	9.4
4		5.4	8.6	9.5
5		8.4	9.5	7.7
6		9.2	8.3	8.8
7		8.3	7.9	10.0
8		7.1	8.2	8.8
9	9.5	10	8.3	9.3
10		9.1	9.8	11.0
11		6.9	9.3	12.0
12		10.0	10.0	10.5
13		8.4	7.9	10.4
14		7.6	7.5	9.7
15	9.8	7.8	6.3	9.5
16		7.6	6.4	13.7
17		7.8	7.1	8.8
18		8.5	6.9	11.0
19	12.0	6.4	7.5	9.3
20	10.5	7.6		10.6
21	8.5	4.5	4.5	8.3
22	10.0	6.7		9.3
23	8.9	7.3	7.5	10.0
24	10.0	8.0		12.0
25	7.3	7.4	6.4	9.8
26		8.4	6.5	9.3
27		8.8	8.9	11.3

However, in order to obtain a $\log M_0/M_L$ relation that holds for a wide range of magnitudes for earthquakes in Greece, we collected the data for 190 earthquakes. These events are listed in the Appendix. The seismic moments have been independently determined mainly by inversion of body or surface waves. Figure 4 shows a plot of $\log(M_0)$ of these earthquakes (black dots) versus M_L (taken from Baba et al., 2000). The $\log M_0/M_L$ pairs for the data set used here are plotted in Figure 4 as open squares. The linear trend is evident,

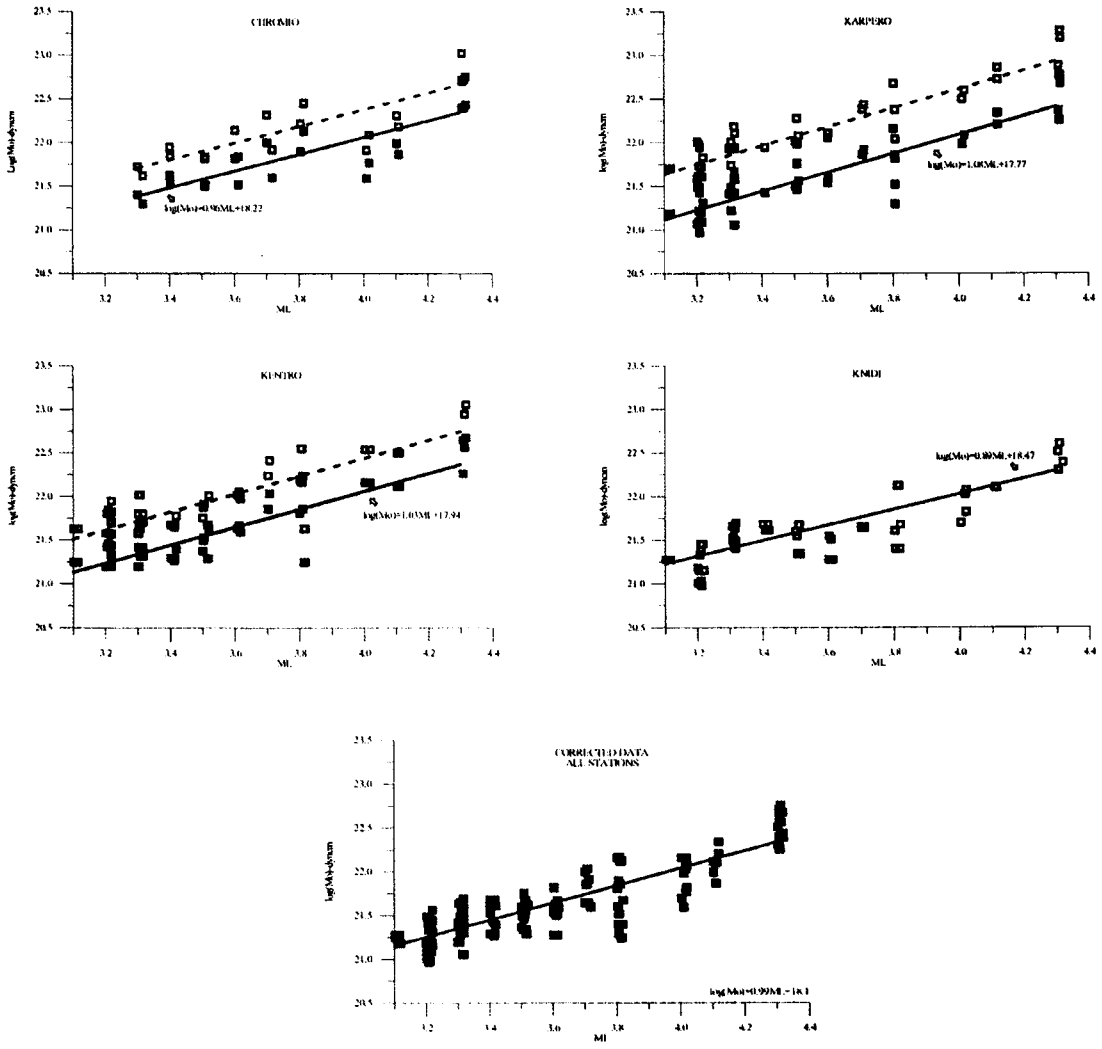

Figure 3. Upper part: Seismic moment, M_0 versus M_L for the magnitude range (3.1 to 4.3), for each station separately. The open squares correspond to M_0 values before the correction for site effect, while the black squares correspond to M_0 values after accounting for the amplification of the low-frequency part of the spectrum, due to the site effect. All observations have been normalized according to the station of Knidi, which is considered as rock. Dashed and straight lines represent the least squares' fit to the data before and after the correction, correspondingly. Lower part: Least squares' fit to all the data. The slope of the line is close to 1 as it is theoretically expected.

at least for $M_L \geq 4.0$. Thus, applying a least squares' fit to the data with $M_L \geq 4.0$, and assuming a slope of 1.5 (Kanamori and Anderson, 1975; Margaris and Papazachos, 1999) we defined the following relation between $\log M_0/M_L$:

$$\log M_0 = 1.5 M_L + (16.52 \pm 0.33) \qquad (7)$$

The relatively larger value of constant b compared to analogous relations proposed for other regions in the world (e.g., b = 15.8 in Aki, 1969; b = 16.0 in Thacher and Hanks, 1973), is probably due to an incorrect calibration of the Wood-Anderson seismograph in Athens (Papazachos et al., 1997; Margaris and Papazachos, 1999).

The least squares' fit to the data (for $M_L \geq 4.0$) is shown as a solid line, while the extrapolation of this relation towards smaller magnitudes is shown as a

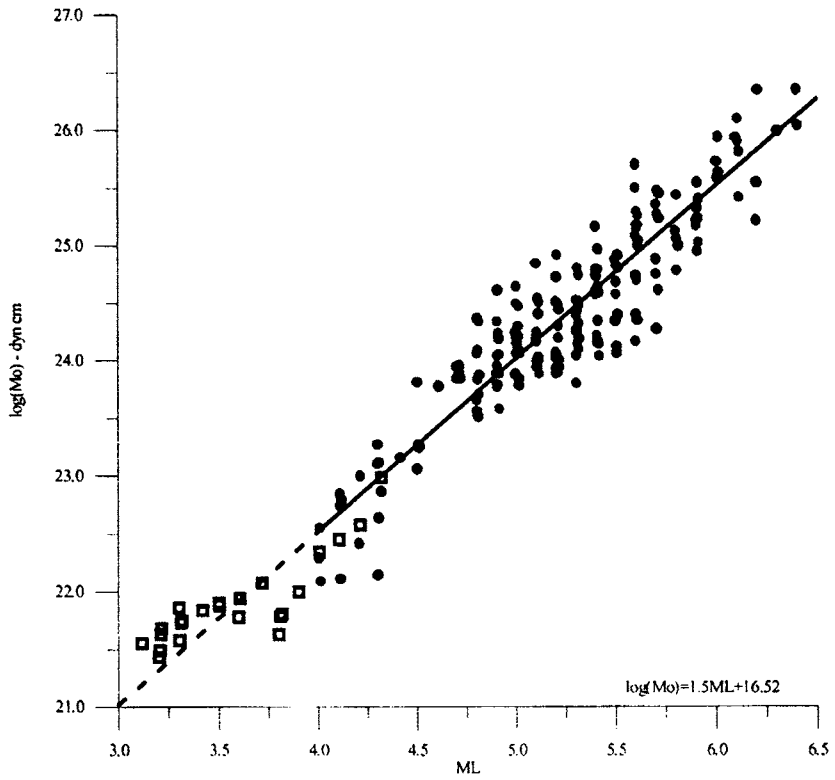

Figure 4. Seismic moment, M_0, versus M_L (according to Baba et al., 2000) for the magnitude range (3.1 to 6.5) for earthquakes in the Aegean Sea and the surrounding area. Solid circles represent observations from 190 earthquakes (listed in the Appendix) while squares are the data from the 27 earthquakes of the present study. The continuous line represents the least squares' fit to the data with $M_L \geq 4.0$. Its extrapolation towards smaller magnitudes is shown as a dashed line.

dashed line. It appears that our data are quite well described by the extrapolation of the relation that holds for larger earthquakes. Nevertheless, a change of slope might exist around $M_L 4.0$, indicating a pattern analogous to that observed for earthquakes in California (Fletcher, 1984). However more data are needed to obtain more convincing conclusions.

Moment versus f_c and f_{max}

The average values of f_c and individual values of f_{max}, against seismic moment are shown in Figure 5. Straight lines indicate the f_c -M_0 relation as proposed by Aki (1967), and the $f_{max} - M_o$ relation describing observed pairs of corresponding values by Papageorgiou and Aki (1983) and Irikura and Yokoi (1984). It appears that our data adequately fit both relations. Earthquakes with $M_0 < \sim 4 \times 10^{21}$ dyn·cm show a deviating trend from the M_0-f_c line by exhibiting an apparently constant f_c. Such a phenomenon has been widely observed and interpreted as a source effect (Bakun et al., 1976; Chouet et al., 1978; Archuleta et al., 1982).

In Figure 5 it is observed that the recordings at the stations of Knidi and Chromio exhibit larger values of f_{max} than the corresponding records in Kentro and Karpero. These differences can either be attributed to near surface attenuation or to amplification phenomena, since Knidi and Chromio both favor amplifications at frequencies higher than ~10 Hz (Theodoulidis et al., 1998). Correlation between f_{max} and resonant peaks at the recording stations was also observed by Theodoulidis and Bard (1998) during an analysis of data from larger Greek earthquakes.

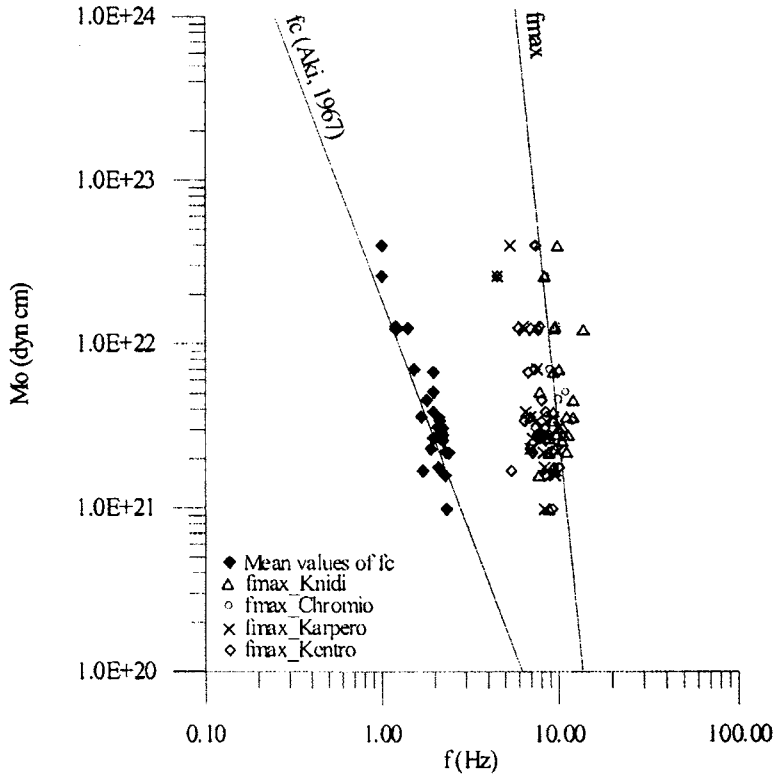

Figure 5. Seismic moment versus f_c and f_{max}. Reference lines correspond to a corner frequency-moment relation proposed by Aki (1967) and to observed pairs of M_0-f_{max} by Papageorgiou and Aki (1983) and Irikura and Yokoi (1984). Our data adequately fit these relations.

Moment versus source radius, r

In Figure 6, the average M_0 is plotted against the average source radius, r. Lines of constant stress drop, determined from equation (4), are also shown in this figure. It appears that source radius is varying very slowly within the examined range of seismic moment. Even though it is hard to claim constant value, the decrease of source radius with decreasing seismic moment is very slow and clearly different from the scaling relation predicted for constant stress drop. The correlation between seismic moment and source radius is relatively poor and thus a link through a relationship is hard to be defined.

Moment versus stress drop, $\Delta\sigma$

In Figure 7, the values of $\log(M_0)$ are plotted against the values of $\log(\Delta\sigma)$. The data exhibit a quite strong correlation between seismic moment and stress drop (R 83%). A least square's fit to the data yields the relation:

$$\log(M_0) = (1.18 \pm 0.11)\log(\Delta\sigma) + (20.63 \pm 0.09) \quad (10^{21} \leq Mo < 10^{23} \text{dyn·cm}) \qquad (8)$$

Stress drop decreases as seismic moment decreases. This is also indicated in the previous figure (Figure 6), where the observations intersect the constant stress drop lines. Archuleta et al. (1982) noticed a similar decrease of stress drop for small magnitude earthquakes ($M_0 \leq 1.0 \times 10^{21}$ dyn·cm). In our case, this decrease appears throughout the entire examined range of seismic moments (up to $M_0 \sim 4.0 \times 10^{22}$ dyn·cm). Furthermore, the values of stress drop consistent with our data are relatively low, ranging from 2 bars to 30 bars (only one earthquake of $M_L = 4.3$ appears to have $\Delta\sigma > 30$ bars). This confirms the low stress drop character of Greek earthquakes, mentioned by many researchers in the past (Kiratzi et al., 1985).

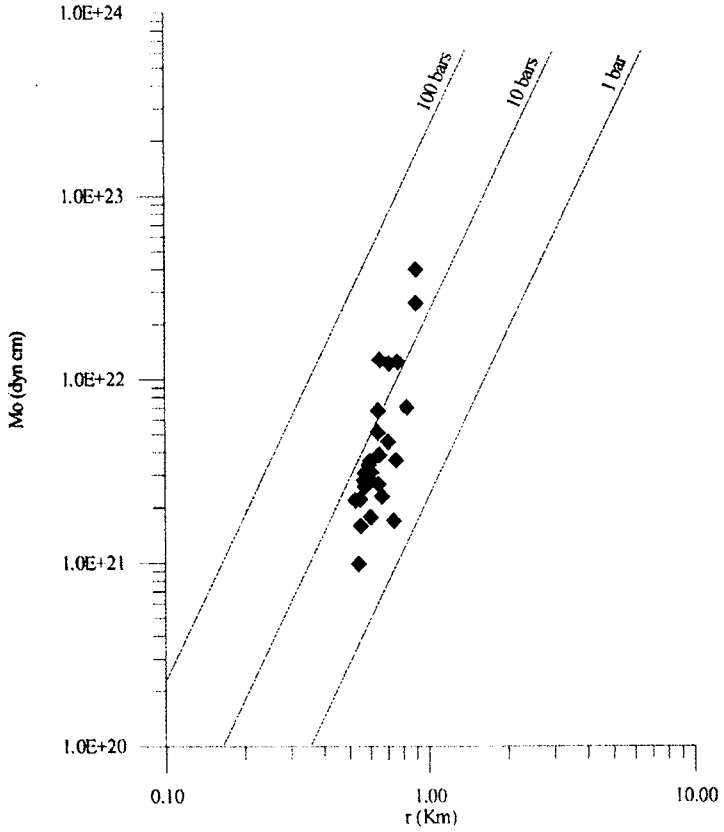

Figure 6. Seismic moment versus source radius. Lines of constant stress drop determined from equation (4) are also indicated.

Moment versus slip, s

Average displacement, s, as a function of seismic moment, is shown in Figure 8. The linear trend is evident, as expected since the radius, r, in equation (5) was found to be nearly constant for this range of magnitudes. A linear least squares' fit to the data gave the relation:

$$\log(M_0) = (1.25 \pm 0.005)\log(s) + (21.87 \pm 0.001) \quad (10^{21} \leq Mo < 10^{23} \text{dyn·cm}) \qquad (9)$$

with a correlation coefficient of 0.92. This relation is applicable only for the moment range that is defined and extrapolation to larger moment should not be applied.

Discussion and conclusions

The S-wave spectral analysis of Brune (1970, 1971), has been applied to 174 strong motion records, in order to determine the source parameters of 27 aftershocks of the May 13, 1995, Kozani-Grevena earthquake (M_w 6.6). The magnitudes of these earthquakes are in the range of $3.1 \leq M_L \leq 4.3$.

Site effects at three out of the four stations used were evident, and a correction was applied to account for the amplification of the low-frequency part of the spectrum at these stations. The effect of the recording site can be a problem especially when strong motion records are used, since accelerographs are usually deployed in urban areas, mostly settled in sedimentary basins (e.g. river valleys). On the other hand, traditional techniques for the estimation of site-effects (e.g. Borcherdt, 1970; Langston, 1979; Nakamura, 1989) are not always effective, either because they use

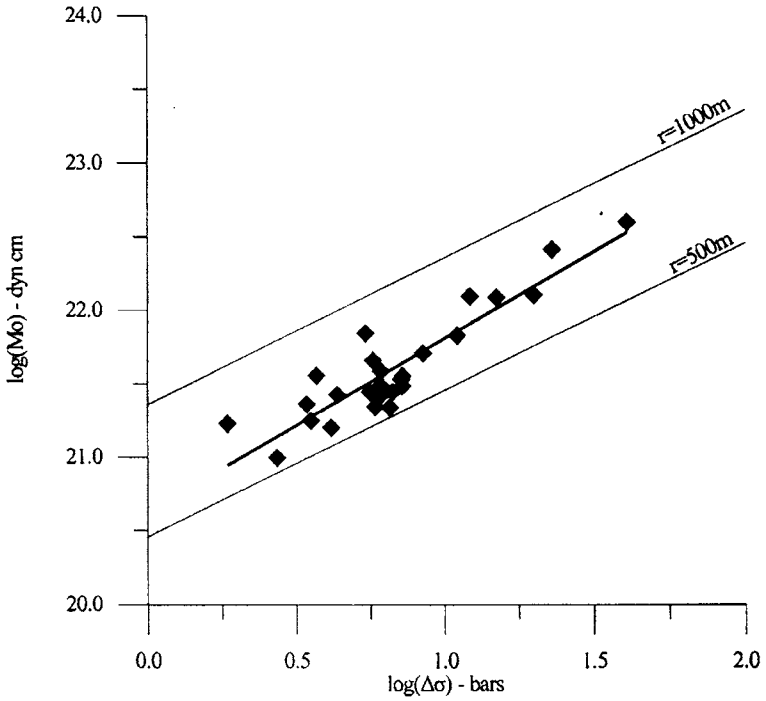

Figure 7. Seismic moment versus stress drop. The straight line is the least squares' fit to the data. Lines of constant source radius are also shown.

reference-site recordings which reveal high-frequency resonance that can affect the choice of corner frequencies, or because they do not give reliable results throughout the entire frequency-range of interest (Bard, 1997). The correction proposed in this study can be applied for an approximate determination of the overestimation of M_0 due to site-effects, in cases where data from a reference rock-site are also available. This correction is statistically estimated from the values of M_0, that are related to the low-frequency part of the spectrum, obtained at different stations and thus it does not affect the choice of corner frequencies.

A $\log M_0/M_L$ relation has been determined using previously published data from 190 earthquakes, which occurred in the Aegean Sea and the surrounding area. A relation of the form:

$$\log M_0 = 1.5M_L + 16.51$$

was found to hold for earthquakes with $M_L \geq 4.0$. An extrapolation of this relation towards smaller magnitudes satisfactorily describes the data of the present study. Thus, this equation can be applied to earthquakes in Greece with magnitude $M_L \geq 3.0$. Nevertheless, one could claim a change of slope around M_L = 4.0. A least squares' fit to the data of the present study results in a slope ~ 1, which could be indicative of a departure from the self-similarity law. However, such a conclusion cannot be ensured by the present data as they concern a specific region and the examined magnitude range is relatively short. More earthquakes with local magnitude 3–5, or even smaller, from different seismogenic regions, should be analyzed and comprised, in order to extract a safe conclusion about the relation between $\log(M_0)$ and M_L at small magnitudes.

Correlation between $\log(M_0)$–$\log(\Delta\sigma)$ and $\log(M_0)$ – log(s) was found to be quite high, while radius, r, appears to decrease very slowly as seismic moment decreases. If this implied minimum source dimension really exists, as proposed by Aki (1984) and is not due to the incapability of surface instruments to detect very high frequency ($f > f_{max}$) waves because of strong attenuation, then close to the minimum source radius, $\Delta\sigma$ also decreases without limit as M_0 decreases. In terms of scaling laws, this is expressed as a difference

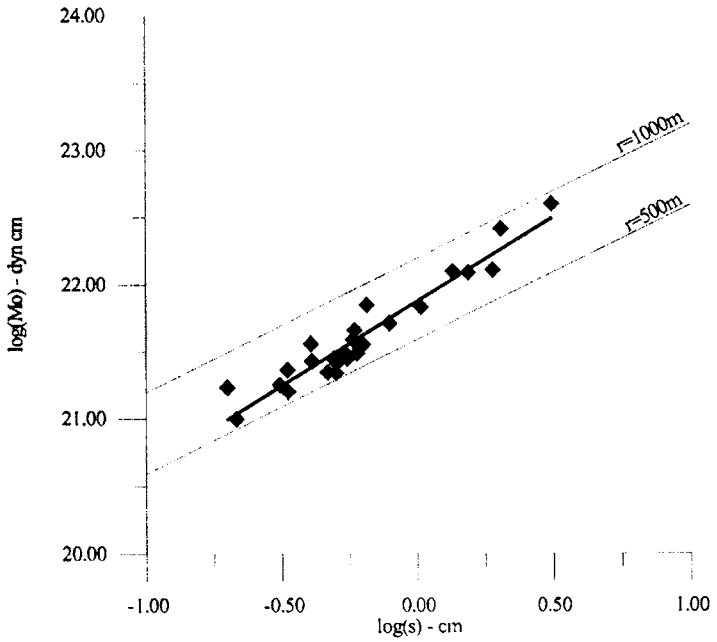

Figure 8. Seismic moment versus average seismic slip. Lines of constant source radius and the least squares' fit to the data (straight line) are also shown.

in stress drop between the analyzed small earthquakes and larger earthquakes.

The corner frequency-moment relation of Aki (1967) adequately fits our data, thus this relation is applicable to the Aegean area as well. This description is much more accurate for earthquakes with $M_0 \geq 4 \times 10^{21}$ dyn·cm, as corner frequencies that correspond to smaller seismic moments revealed a roughly constant value. Finally, the determined values of f_{max} were found to be in good agreement with previous observations, which included data from larger earthquakes (Papageorgiou and Aki, 1983; Irikura and Yokoi, 1984). Small but systematic differences were observed between the values obtained at different stations. These differences can either due to near surface attenuation or resonant peaks at high frequencies at the recording sites.

The empirical scaling relations determined here are only applicable for the magnitude ranges that they were defined (for $M_L < 4.0$). We now comprise a database for the earthquakes in Greece to systematically work on applicability of scaling relations to different magnitude ranges.

It should be also mentioned that this work could be useful in strong motion simulation methods that use scaling-laws between small and large earthquakes (e.g. the Empirical Green's Function method). For example, it appears that scaling laws that are based on the assumption of constant stress-drop can not be used in the area of Kozani, at least if an earthquake of magnitude $M_L \leq 4.0$ is to be treated as an empirical Green's function. Revised relations should be used to encounter differences between small and large earthquakes.

Acknowledgements

Thanks are due to Assist. Prof C.B. Papazachos for offering valuable advice. This work was partly supported by the Science for Peace Project (SfP 972342-Seis-Albania), by Egnatia Odos S.A. (Contract No.: 0000/406/GD/A01/10-11-1999) and by OASP (Greece) (Contract 20246/2000).

References

Aki, K., 1967, Scaling law of seismic spectrum, *J. Geophys. Res.* **72,** 1217–1231.

Aki, K., 1969, Analysis of the seismic coda of the local earthquakes as scattered waves, *J. Geophys. Res.* **74,** 615–631.

Aki, K., 1984, Asperities, barriers, characteristic earthquakes and strong motion prediction, *J. Geophys. Res.* **89,** 5867–5872.

Aki, K., 1987, Magnitude-frequency relation for small earthquakes: A clue to the origin of f_{max} of large earthquakes, *J. Geoph. Res.* **92,** 1349–1355.

Anderson, J. and Hough, S., 1984, A model for the shape of the Fourier amplitude spectrum of acceleration at high frequencies, *Bull. Seism. Soc. Am.* **74,** 1969–1993.

Anderson, H. and Jackson, J., 1987, Active tectonics of the Adriatic region, *Geophys. J. R. Astr. Soc.* **91,** 937–983.

Andrews, D.J., 1986, Objective determination of source parameters and similarity of earthquakes of different size, In: Das, S., Boatwright, J., and Scholtz, S.H. (eds), *Earthquake Source Mechanics*, Maurice Ewing Series 6, AGU, Washington, D.C., pp. 259–267.

Archuleta, R.J. and Hartzell, S.H., 1981, Effects of fault finiteness on near-source ground motion, *Bull. Seism. Soc. Am.* **71,** 939–957.

Archuleta, R.J., Granswick, Å., Mueller, C. and Spudich, P., 1982, Source parameters of the 1980 Mammoth lakes, California, earthquake sequence, *J. Geophys. Res.* **87,** 4595–4607.

Baba, A., Papadimitriou, E.E., Papazachos, B.C., Papaioannou, Ch.A. and Karakostas, B.G., 2000, Unified local magnitude scale for earthquakes of South Balkan area, *Pageoph* **157,** 765–783.

Baker, C., Hatzfeld, D., Lyon-Caen, H., Papadimitriou, E. and Rigo, A., 1997, Earthquake mechanisms of the Adriatic Sea and western Greece, *Geophys. J. Int.* **131,** 559–594.

Bakun, W.H., Bufe, C.G. and Stewart, R.M., 1976, Body wave spectra of central California earthquakes, *Bull. Seism. Soc. Am.* **66,** 439–459.

Bard, P.-Y., 1997, Local effects on strong ground motion: basic physical phenomena and estimation methods for microzoning studies, In: 'SERINA-Seismic Risk: An Integrated Seismological, Geotechnical and Structural Approach', ITSAK, Thessaloniki, 21-27 September 1997: pp. 227–299.

Barker, G. and Langston, C., 1981, Moment tensor inversion of complex earthquakes, *Geophys. J. R. Astr. Soc.* **68,** 777–803.

Bezzeghoud, M., 1987, *Inversion et analyse spectrale des ondes*, P.Ph.D. Thesis, University Paris VII, 232 pp.

Boore, D., Sims, J., Kanamori, H. and Harding, S., 1981, The Montenegro, Yugoslavia, earthquake of April 15, 1979: source orientation and strength, *Phys. Earth Planet. Interiors* **27,** 133–142.

Borcherdt, R.D., 1970, Effects of local geology on ground motion near San Francisco Bay, *Bull. Seism. Soc. Am.* **60,** 29–61.

Bour, M., 1989, *Estimation automatique de f_{max} sur des donnees accelerometriques Italiennes relation avec les parameters de source et de site*, Rapport de stage de DEA, LGIT-IRIGM, Univ. Joseph Fourier, pp. 80 (in French).

Braunmiller, J. and Nabelek, J., 1996, Geometry of continental normal faults: Seismological constraints, *J. Geophys. Res.* **10,** 3045–3052.

Brune, J.N., 1968, Seismic moment, seismicity, and rate of slip along major fault zones, *J. Geophys. Res.* **73,** 777–784.

Brune, J.N., 1970, Tectonic stress and the spectra of seismic shear waves from earthquakes, *J. Geophys. Res.* **75,** 4997–5009.

Brune, J.N., 1971, Correction, *J. Geophys. Res.* **76,** 5002.

Burton, P.W., Makropoulos, K.C., McGonigle, R.W., Ritchie, M.E.A., Main, I.G., Kouskouna, V. and Drakopoulos, J., 1991, *Contemporary seismicity on the Nea Ankhialos fault, eastern Greece: fault parameters of major and minor earthquakes*, Technical Report WL/91/29, Seismology Series, British Geological Survey, 55 pp.

Chouet, B., Aki, K. and Tsujiura, M., 1978, Regional variation of the scaling law of earthquake source spectra, *Bull. Seism. Soc. Am.* **68,** 49–80.

Chouliaras, G. and Stavrakakis, G.N., 1997, Seismic source parameters from a new dial-up network in Greece, *Pageoph.* **150,** 91–111.

Del Pezzo, E., De Natale, G., Martini, M. and Zollo, G., 1987, Source parameters of micro-earthquakes at Phlegraean Fields (Southern Italy) volcanic area, *Phys. Earth Planet. Interiors* **47,** 25–42.

Eyidogan, H. and Jackson, J., 1985, A seismological study of normal faulting in the Demirci, Alasehir and Gediz earthquakes of 1969–70 in western Turkey: Implications for the nature and geometry of deformation in the continental crust, *Geophys. J. R. Astr. Soc.* **81,** 569–607.

Fletcher, J., Boatwright, J., Haar, L., Hanks, T. and McGaar, A., 1984, Source parameters for aftershocks of the Oroville, California, earthquake, *Bull. Seism. Soc. Am.* **74,** 1101–1123.

Hanks, T., 1979, b values and $\omega^{-\gamma}$ seismic source models: Implication for tectonic stress variation along active crustal fault zones and the estimation of high frequency strong ground motion, *J. Geophys. Res.* **84,** 2235–2242.

Hanks, T.C., 1982, f_{max}, *Bull. Seism. Soc. Am.* **72,** 1867–1879.

Hatzfeld, D., Kementzetzidou, D., Karakostas, V., Ziazia, M., Nothard, S., Diagourtas, D., Deschamps, A., Karakaisis, G., Papadimitriou, P., Scordillis, M., Smith, R., Voulgaris, N., Kiratzi, A., Makropoulos, K., Bouin, M.P. and Bernard, P., 1996, The Galaxidi Earthquake of 18 November 1992: A possible asperity within the normal fault system of the gulf of Corinth (Greece), *Bull. Seism. Soc. Am.* **86,** 1987–1991.

Ioannidou, H., 1989, *Seismic Source Parameters Determined by the Inversion of Body Waves: Greece and the Surrounding Area*, Ph.D. Thesis, Athens University, 185 pp.

Irikura, K. and Yokoi, T., 1984, Scaling law of seismic source spectra for the aftershocks of 1983 Central-Japan-Sea earthquake, *Abstracts of the Seism. Soc. of Japan* **No 1.**

Jackson, J. and McKenzie, D.P., 1984, Active tectonics of the Alpine Himalayan Belt between western Turkey and Pakistan, *Geophys. J. R. Astr. Soc.* **77,** 185–264.

Kanamori, H. and Anderson, D.L., 1975, Theoretical basis of some empirical relations in seismology, *Bull. Seism. Soc. Am.* **65,** 1073–1095.

Keilis-Borok, V., 1959, On the estimation of the displacement in an earthquake source and of source dimensions, *Ann. di Geofis.* **12,** 205–214.

Kiratzi, A.A., 1991, The focal mechanism of the 25/5/1971 (M = 6.1) aftershock of the Gediz (Turkey) earthquake, *Publ. of the Geophys. Lab. of Thessaloniki* **No. 8,** 45–47.

Kiratzi, A.A., Karakaisis, G.F., Papadimitriou, E.E. and Papazachos, B.C., 1985, Seismic source-parameter relations for earthquakes in Greece, *Pageoph* **123,** 28–41.

Kiratzi, A. and Langston, C., 1989, Estimation of earthquake source parameters of the May 4, 1972 event of the Hellenic arc by the inversion of waveform data, *Phys. Earth Planet. Interiors* **57,** 225–232.

Kiratzi, A., Wagner, G. and Langston, C., 1990, Source parameters of some large earthquakes in Northern Aegean determined by body waveform modeling, *Pageoph.* **135,** 515–527.

Kulhanek, O. and Meyer, K., 1983, *Spectral Study of the June 20, 1978, Thessaloniki Earthquake*, Seism. Section, Uppsala University, 25 pp.

Langston, C.A., 1979, Structure under Mount Rainier, Washington, inferred from teleseismic body waves, *J. Geophys. Res.* **84,** 4749–4762.

Liotier, Y., 1989, *Modelisation des ondes de volume des seismes de l'arc Ageen*, DEA de l'Universite Joseph Fourier, Grenoble, France.

Louvari, E., 2000, *Detailed Seismotectonic Study of Greece and its Surroundings based on Fault Plane Solutions of Small Earthquakes*, Ph.D. Thesis, University of Thessaloniki, 370 pp. (in Greek).

Margaris, B.N. and Papazachos, C.B., 1999, Moment-magnitude relations based on strong-motion records in Greece, *Bull. Seism. Soc. Am.* **89,** 442–455.

Melis, N., Burton, P.W. and Brooks, M., 1995, Coseismic crustal deformation from microseismicity in the Patras area, western Greece, *Geophys. J. Int.* **122,** 815–836.

Meuller, C.S. and Cranswick, E., 1985, Source parameters from locally recorded aftershocks of the 9 January 1982 Miramichi, New Brunswick, earthquake, *Bull. Seism. Soc. Am.* **75,** 337–360.

Modiano, T. and Hatzfeld, D., 1982, Experimental study of the spectral content for shallow earthquakes, *Bull. Seism. Soc. Am.* **72,** 1739–1758.

Nakamura, Y., 1989, A method for dynamic characteristics estimation of subsurface using microtremors on the ground surface, *Q. Rept. Railway. Tech. Res. Inst.* **30**(1), 25–33.

North, R., 1977, Seismic moments, source dimensions and stress associated with earthquakes in the Mediterranean and Middle East, *Geophys. J. R. Astr. Soc.* **49,** 137.

Papadimitriou, E., 1993, Focal mechanism along the convex side of the Hellenic arc, *Bollettino de Geofisica Teorica ed Applicata* **XXXV,** 401–426.

Papadimitriou, P., 1988, *Etude de la structure du manteau supérieur de l' Europe et modélisation des ondes de volume engendrées par des séismes Egéens*, Ph.D. Thesis, University of Paris VII, 211 pp.

Papageorgiou, A.S., 1988, On two characteristic frequencies of acceleration spectra: patch corner frequency and f_{max}, *Bull. Seism. Soc. Am.* **78,** 509–529.

Papageorgiou, A.S. and Aki, K., 1983, A specific barrier model for the quantitative description of inhomogeneous faulting and the prediction of strong ground motion. I. Description of the model, *Bull. Seism. Soc. Am.* **73,** 693–722.

Papazachos, B.C., Kiratzi, A.A. and Karacostas, B.G., 1997, Toward a homogeneous moment-magnitude determination for earthquakes in Greece and the surrounding area, *Bull. Seism. Soc. Am.* **87,** 474–483.

Pavlides, S.B., Zouros, N.C., Chatzipetros, A.A., Kostopoulos, D.S. and Mountrakis, D.M., 1995, The 13th May 1995 Western Macedonia, Greece, Kozani Grevena earthquake; preliminary results, *Terra Nova* **7,** 544–549.

Pitilakis, K. (scientific responsible), et al., 1996, *Seismic hazard assessment, geotechnical survey and site response analysis for residential applicability of settlements in the Kozani-Grevena meizoseismal area*, Final Report, pp. 83 (in Greek).

Randall, M.J., 1973, The spectral theory of seismic sources, *Bull. Seism. Soc. Am.* **63,** 1133–1144.

Scherbaum, F., 1994, *Basic Concepts in Digital Signal Processing for Seismologists*, Springer-Verlag Publications, pp. 158.

Seed, H.B., Murarka R., Lysmer J. and Idriss, I.M., 1976, Relationships of maximum acceleration, maximum velocity, distance from source, and local site conditions for moderately strong earthquakes, *Bull. Seism. Soc. Am.* **66,** 1323–1342.

Street, R.N., Hermann R.B. and Nuttli, O.W., 1975, Spectral characteristics of the Lg wave generated by Central United States earthquakes, *Geophys. J. R. Astr. Soc.* **41,** 51–63.

Taymaz, T. and Price, S., 1992, The 1971 May 12 Burdur earthquake sequence, SW Turkey: a synthesis of seismological and geological observations, *Geophys. J. Int.* **108,** 589–603.

Taymaz, T., Jackson, J. and Westaway, R., 1990, Earthquake mechanics in the Hellenic Trench near Crete, *Geophys. J. Int.* **102,** 695–731.

Taymaz, T., Jackson, J. and McKenzie, D., 1991, Active tectonics of the north and central Aegean Sea, *Geophys. J. Int.* **106,** 433–490.

Thatcher, W. and Hanks, T.C., 1973, Source parameters of Southern California earthquakes, *J. Geophys. Res.* **78,** 8547–8576.

Theodulidis, N. and Bard, P.-Y., 1998, *Dependence of f_{max} on site geology: A preliminary study of Greek strong-motion data*, Proc. 11th ECEE, **1**, September 6-11, 1998, pp. 269–274.

Theodoulidis, N., Lekidis V., Margaris B., Papazachos C., Papaioannou Ch. and Dimitriou, P., 1998, Seismic hazard assessment and design spectra for the Kozani-Grevena region (Greece) after the earthquake of May 13, 1995, *J. Geodynamics* **26**(2-4), 375–391.

Appendix

Parameters of the events with $4.0 \leq M_L \leq 6.5$ used to determine the M_0-M_L relation applicable to Greece.

Date (y/m/d)	Origin time	Lat. (°N)	Long. (°E)	h (Km)	M_L	M_0 (dyn·cm)	Reference
640411	16:00:43	40.30	24.80	1.0	5.2	3.20e24	1
640429	04:21:05	39.20	23.70	20.0	5.5	2.20e24	1
641006	14:31:23.0	40.30	28.20	14.0	6.4	1.10e26	1, 2
650309	17:57:54.0	39.30	23.80	7.0	5.9	1.60e25	1, 2
650405	03:12:55	37.70	22.00	34.0	5.6	1.50e25	1
650427	14:09:06.0	35.60	23.50	13.0	5.9	1.04e25	1, 3
650613	20:01:51.0	37.80	29.30	2.0	5.2	8.20e24	1
650706	03:18:42.0	38.40	22.40	10.0	6.2	1.63e25	4, 5, 6
651220	00:08:16	40.20	24.80	33.0	5.2	5.30e24	1
660205	02:01:45.0	39.10	21.70	11.0	5.9	1.48e25	6, 7
660509	00:42:53.0	34.40	26.40	16.0	5.4	2.20e24	8
661029	02:39:25.0	38.90	21.10	15.0	5.6	5.05e24	1, 6
670501	07:09:02.0	39.50	21.20	10.0	5.8	1.12e25	6, 7
671130	07:23:50.0	41.40	20.40	9.0	6.1	8.60e25	1, 6
680530	17:40:26	35.40	27.90	27.0	5.6	1.20e25	1
681205	07:52:11	36.60	26.90	31.0	5.6	1.80e25	1
690114	23:12:06	36.10	29.20	22.0	6.0	5.30e25	1
690323	21:08:42.0	39.10	28.50	8.0	5.8	9.80e24	9
690325	13:21:34.0	39.20	28.40	8.0	5.7	1.85e25	9, 10
690328	01:48:29.0	38.50	28.50	8.0	6.2	3.50e25	9, 11
690612	15:13:31.0	34.40	25.00	19.0	5.6	9.90e24	5, 8
690708	08:09:13.0	37.50	20.30	10.0	5.7	5.60e24	6, 12
700408	13:50:28.7	38.30	22.60	9.0	5.4	1.45e25	3, 4, 5
700416	10:42:23.7	38.97	29.92	8.0	5.3	2.70e24	9
700419	13:29:37.9	39.00	29.80	9.0	5.6	1.94e25	9
700423	09:01:27	39.10	28.60	28.0	5.4	3.80e24	1
710512	06:25:13.0	37.57	29.70	12.0	5.8	6.00e24	13
710512	12:57:22.7	37.60	29.60	12.0	5.6	2.50e24	13
710525	05:43:27.7	39.07	29.67	6.0	5.7	7.60e24	9, 14
720504	21:39:57.0	35.10	23.60	40.0	6.1	2.60e25	8, 15
720917	14:07:15.0	38.30	20.30	8.0	5.8	1.31e25	5, 12, 15
731104	15:52:13.9	38.90	20.51	23.0	5.4	6.10e24	1
731129	10:57:44.0	35.20	23.80	18.5	5.5	6.40e24	5, 8
750327	05:15:08.4	40.34	26.14	15.0	5.7	2.83e25	2, 5
760511	16:59:45.0	37.40	20.40	13.0	5.9	2.08e25	6, 12
770818	09:27:41.0	35.30	23.50	38.0	5.2	2.00e24	8
770911	23:19:19.0	34.90	23.00	19.0	5.9	2.49e25	5, 8
780523	23:34:12.3	40.70	23.30	8.0	5.4	6.20e24	6, 16
780620	20:03:24.0	40.73	23.25	7.0	6.0	4.25e25	10, 11, 16, 17, 18
790409	02:10:21.1	41.90	19.03	9.0	5.0	1.73e24	19
790415	14:43:07.9	42.22	18.69	8.0	5.7	4.10e24	6, 20
790515	06:59:23.0	34.60	24.50	35.0	5.4	3.90e24	8
790524	17:23:20.0	42.15	18.71	6.0	5.9	1.63e25	4, 6
790614	11:44:45.8	38.80	26.60	8.0	5.5	6.70e24	2, 21
790615	11:34:17.0	34.90	24.20	40.0	5.1	3.50e24	8
790616	18:42:00	38.80	26.60	15.0	4.8	1.20e24	21
790718	13:12:03	39.70	28.70	15.0	5.2	1.15e24	21
790723	11:41	35.50	26.40	11.0	5.1	3.20e24	21

Date (y/m/d)	Origin time	Lat. (°N)	Long. (°E)	h (Km)	M_L	M_0 (dyn·cm)	Reference
800502	05:31:09.6	36.35	29.39	22.0	5.3	3.34e24	19
800709	02:11:57.0	39.28	23.11	10.0	6.0	8.67e25	21
800710	19:39:02.5	39.28	23.01	15.0	5.0	3.08e24	21
800811	09:15:58.3	39.27	22.66	17.0	4.7	7.46e23	21
810224	20:53:37.0	38.16	22.88	8.6	6.3	9.76e25	11, 21
810225	02:35:54.0	38.10	23.05	6.7	5.9	3.50e25	11, 21
810304	21:58:07.0	38.18	23.23	7.0	5.8	2.70e25	2, 21
810307	11:34:43.9	38.19	23.32	15.0	5.1	1.47e24	21
810310	15:16:18.1	39.31	20.74	7.0	5.3	1.54e24	19, 21
810624	18:41:27.7	37.87	20.12	5.3	5.2	8.65e23	21
810628	17:20:23.0	37.81	20.06	14.0	5.5	2.44e24	19, 21
811219	14:10:51.0	39.20	25.20	6.0	6.4	2.24e26	21, 22
811227	17:39:14.5	38.90	24.90	6.0	6.0	3.82e25	2, 21
811229	08:00:45.0	38.80	24.77	10.0	5.4	1.37e24	21
820118	19:27:25.0	39.80	24.40	7.0	6.1	7.97e25	2, 21
820622	03:04:29.4	37.16	21.27	40.0	5.7	1.86e24	21
820817	22:22:20.0	33.70	22.90	39.0	5.7	3.00e25	8
821116	23:41:21.4	40.90	19.60	17.0	5.3	2.45e24	6, 21
830117	12:41:31.0	38.10	20.20	11.0	6.2	2.22e26	12, 21
830119	00:02:14.0	38.20	20.30	9.1	5.5	4.79e24	19, 21
830131	15:27:01.2	38.18	20.39	12.0	5.3	1.82e24	19, 21
830221	00:13:07.6	37.89	20.10	26.0	5.1	9.73e23	21
830323	23:51:06.3	38.33	20.22	15.0	5.7	2.23e25	1
830324	04:17:31.7	38.09	20.29	18.0	5.1	1.44e24	19, 21
830514	23:13:47.9	38.44	20.33	13.0	5.0	1.97e24	19
830705	12:01:27.0	40.32	27.22	10.0	5.9	8.87e24	4, 21
830714	02:54:19.6	35.67	21.81	17.0	5.2	1.10e24	19, 21
830826	12:52:09.8	40.51	23.92	14.0	4.5	6.41e23	21
831010	10:17:00.7	40.23	26.80	11.0	5.4	1.48e24	19, 21
831021	20:34:49.1	40.13	29.38	14.0	5.1	1.64e24	21
840211	08:02:51.0	38.37	22.10	3.0	5.1	3.35e24	19, 21
840506	09:12:02.3	38.77	25.64	9.0	4.9	1.71e24	19, 21
840617	07:48:02.6	38.86	25.72	23.0	5.3	6.24e23	21
840621	10:43:46.0	35.40	23.30	39.0	5.9	1.70e25	8, 21
840709	18:57:09.7	40.69	21.82	10.0	4.9	7.59e23	21
850116	23:35:59.1	40.67	19.22	17.0	5.0	7.50e23	19
850421	08:49:40.8	35.68	22.20	36.0	5.1	9.97e23	21
850430	18:14:12.7	39.30	22.80	11.0	5.3	3.00e24	2, 21
850523	16:02:22.7	36.60	22.22	39.0	4.7	8.70e23	21
850907	10:20:50.0	37.50	21.20	29.0	5.2	1.55e24	19, 21
850927	16:39:48.0	34.50	26.60	38.0	5.0	4.40e24	8, 21
850928	14:50:16.6	41.59	22.22	20.0	4.7	8.97e23	21
851109	23:30:42.3	41.24	23.93	18.0	4.9	7.55e23	21
851121	21:57:14.5	41.70	19.30	8.0	5.3	5.55e24	19, 21
860303	01:24:05.7	41.95	20.27	23.0	4.8	3.23e23	21
860325	01:41:35.7	38.40	25.10	6.0	5.2	2.75e24	19, 21
860329	18:36:38.3	38.37	25.17	14.0	5.3	1.25e24	19
860522	19:52:19.5	34.51	26.59	30.0	4.8	2.16e24	21
860608	04:55:01.6	36.07	21.51	29.0	4.6	5.99e23	21
860913	17:24:35.0	37.10	22.20	8.0	5.5	8.16e24	6, 21

Date (y/m/d)	Origin time	Lat. (°N)	Long. (°E)	h (Km)	M_L	M_0 (dyn·cm)	Reference
861002	10:12:39.8	34.63	28.36	10.0	4.9	8.95e23	21
861011	09:00:12.3	37.91	28.53	9.0	5.5	3.76e24	19, 21
870227	23:34:53.8	38.42	20.36	13.0	5.4	4.36e24	19, 21
870412	02:47:18.3	35.43	23.43	33.0	4.9	5.90e23	21
870610	14:50:11.2	37.17	21.39	27.0	5.0	1.25e24	19, 21
880109	01:02:47.3	41.16	19.68	30.0	5.1	6.99e24	19, 21
880424	20:49:35.1	40.90	28.11	19.0	5.1	1.04e24	21
880518	05:17:42.2	38.36	20.42	23.0	5.3	1.10e24	19, 21
880905	20:03:23.8	34.51	26.65	12.0	4.7	8.83e23	21
881016	12:34:06.3	37.95	20.90	29.0	5.5	7.47e24	21
881120	21:01:05.8	35.29	28.67	10.0	5.0	1.61e24	21
890224	00:40:34.9	37.76	29.44	17.0	4.9	1.11e24	21
890317	05:42:51.8	34.64	25.59	17.0	4.9	4.06e24	21
890319	05:36:59.2	39.27	23.51	10.0	5.6	1.44e24	21
890328	13:29:11.2	34.06	24.68	33.0	4.9	2.16e24	21
890427	23:06:52.6	37.10	28.20	7.0	5.0	1.56e24	19, 21
890428	13:30:19.8	37.06	28.01	10.0	5.1	1.74e24	19, 21
890607	19:45:53.6	38.05	21.63	25.0	4.7	6.95e23	21
890614	18:06:37.6	34.30	26.10	10.0	4.8	2.29e24	21
890820	18:32:30.8	37.26	21.14	22.0	5.4	5.40e24	19, 21
890824	02:13:14.2	37.94	20.14	16.0	5.2	7.70e23	19, 21
890905	06:52:30.0	40.20	25.16	10.0	4.9	1.54e24	21
900616	02:16:20.0	39.18	20.54	7.0	5.5	2.50e24	19, 21
900709	11:22:16.4	34.90	26.60	9.0	5.0	1.14e24	19, 21
900718	11:29:25.5	37.04	29.51	14.0	5.3	1.81e24	19, 21
901221	06:57:43.0	40.91	22.36	16.0	5.7	1.70e25	6, 21
910319	12:09:23.4	34.80	26.30	12.0	5.3	2.51e24	19, 21
910626	11:43:33.9	38.34	21.04	22.0	4.7	7.80e23	19, 21
911018	14:04:54.1	35.76	28.64	33.0	4.8	4.49e23	21
920123	04:24:18.7	38.40	20.57	9.0	5.0	2.96e24	19, 21
920320	05:37:25.7	36.65	24.51	15.0	4.8	6.80e23	21
920430	11:44:40.0	35.10	26.60	7.0	5.6	5.41e24	19, 21
920723	20:12:44.9	39.81	24.40	8.0	5.0	1.41e24	19, 21
921106	20:06:02.3	38.02	26.97	6.0	5.6	1.09e25	19
921106	19:08:08.9	38.08	26.95	17.0	5.6	1.41e25	21
921118	21:10:42.8	38.34	22.44	7.4	5.3	6.30e24	21, 23
930305	06:55:08.7	37.15	21.44	37.0	5.1	7.58e23	21
930326	11:58:18.4	37.66	21.30	15.0	5.0	1.61e24	21
930613	23:26:40.9	39.28	20.49	9.0	5.4	1.08e24	19, 21
930714	12:31:49.2	38.17	21.77	19.0	5.1	2.52e24	19, 21
931104	05:18:36.6	38.39	21.99	10.0	4.8	1.13e24	21
940111	07:22:51.8	35.83	21.83	14.0	5.4	1.61e24	19, 21
940128	15:45:25.9	38.67	27.48	14.0	5.3	1.37e24	19, 21
940225	02:30:49.5	38.76	20.56	9.0	5.3	1.76e24	19, 21
940416	23:09:34.1	37.36	20.63	22.0	5.3	2.09e24	19, 21
940524	02:05:39.3	38.83	26.49	10.0	5.6	2.22e24	19, 21
950404	17:10:09.8	40.62	23.68	7.0	4.1	6.14e22	24
950503	21:36:54.3	40.58	23.68	13.0	4.3	1.30e23	24
950503	21:43:27.4	40.62	23.67	20.0	4.5	1.13e23	24
950504	00:34:10.7	40.54	23.63	12.0	5.0	6.80e23	19, 24
950513	08:47:15.0	40.13	21.67	12.0	6.1	1.25e26	19, 21, 24

Date (y/m/d)	Origin time	Lat. (°N)	Long. (°E)	h (Km)	M_L	M_0 (dyn·cm)	Reference
950508	05:11:09.1	38.32	22.14	21.0	4.0	3.51e22	24
950513	18:06:01.2	40.19	21.73	11.0	4.5	1.78e23	24
950514	02:47:00.6	40.12	21.61	5.0	4.5	1.74e23	24
950514	05:59:17.0	40.08	21.58	5.0	4.3	1.86e23	24
950514	09:45:42.0	40.15	21.76	5.0	4.3	1.39e22	24
950514	21:31:13.1	40.06	21.70	5.0	4.3	1.38e22	24
950515	04:13:57.3	40.06	21.68	5.0	5.0	6.08e23	24
950516	23:00:41.9	40.03	21.63	5.0	4.3	1.27e23	24
950516	23:57:28.6	40.09	21.70	5.0	4.6	5.89e23	24
950517	04:14:26.3	40.07	21.69	5.0	5.1	8.65e23	24
950519	06:48:50.4	40.10	21.62	5.0	4.8	3.63e23	24
950528	19:56:41.0	38.38	21.96	5.0	4.1	5.40e22	24
950530	12:06:42	40.05	21.64	4.0	4.1	1.28e22	25
950530	14:30:02	39.97	21.55	6.2	4.0	1.22e22	25
950606	04:35:59	40.13	21.58	6.5	4.2	2.59e22	25
950611	18:51:48.6	39.99	21.67	5.0	4.3	4.26e22	24, 25
950615	00:15:49.1	38.36	22.23	7.2	5.6	5.02e25	21, 24
950615	00:30:52.9	38.33	21.93	5.0	5.2	8.40e23	24
950615	04:51:20.8	38.26	22.15	19.0	4.1	6.86e22	24
950619	03:54:00.3	40.07	21.89	5.0	4.4	1.43e23	24
950705	18:24:38.1	38.38	22.10	5.0	4.2	9.87e22	24
950710	18:12:39.0	38.40	22.08	17.0	4.0	1.94e22	24
950717	23:18:16.3	40.14	21.61	7.0	4.9	3.79e23	24
950718	07:42:55.0	40.14	21.63	5.0	4.3	7.18e22	24
950719	18:23:15.8	40.11	21.71	7.0	4.5	1.83e23	24
951210	03:27:49.6	34.76	23.99	24.0	4.8	7.40e23	19
960201	17:57:55.9	37.70	19.78	5.0	5.2	3.05e24	19
960402	07:59:25.6	37.89	26.88	15	5.0	1.14e24	19
960726	18:55:50.4	40.05	20.68	1	4.9	6.14e23	19
970516	07:00:49.7	41.02	20.33	5	5.5	1.15e24	19
970727	10:07:52.3	35.28	21.00	40	5.2	1.01e24	19
971013	13:39:39.2	36.41	22.18	6	5.6	3.14e25	19
971105	12:22:58.4	34.91	24.02	15	4.7	6.93e23	19
971105	21:10:28.3	38.34	22.31	3	4.9	1.09e24	19
971114	21:38:52.7	38.80	25.87	25	5.4	4.04e24	19
971118	13:07:36.9	37.26	20.49	5	6.1	6.46e25	19
980110	19:21:54.3	37.12	20.73	5	5.2	1.03e24	19
980429	03:30:37.1	35.99	21.98	5	5.5	1.31e24	19
980501	04:00:08.1	37.20	20.43	5	4.8	5.07e23	19
981006	12:27:43.3	37.19	21.13	5	5.2	7.79e23	19
990907	11:56:50.5	38.15	23.62	30	5.4	9.22e24	19

1. North (1977), 2. Taymaz et al. (1991), 3. Liotier (1989), 4. Papadimitriou (1988), 5. Ioannidou (1989), 6. Baker et al. (1997), 7. Anderson and Jackson (1987), 8. Taymaz et al. (1990), 9. Eyidogan and Jackson (1985), 10. Jackson and McKenzie (1984), 11. Braunmiller and Nabelek (1996), 12. Papadimitriou (1993), 13. Taymaz and Price (1992), 14. Kiratzi (1991), 15. Kiratzi and Langston (1989), 16. Bezzeghoud (1987), 17. Kulhanek and Meyer (1983), 18. Barker and Langston (1981), 19. Louvari (2000), 20. Boore et al. (1981), 21. CMT Harvard determinations, 22. Kiratzi et al. (1990), 23. Hatzfeld et al. (1996), 24. Chouliaras and Stavrakakis (1997), 25. This study.